RSC Advances

ROYAL SOCIETY OF CHEMISTRY

www.rsc.org/advances

Effect of solid loading on properties of reaction bonded silicon carbide ceramics by gelcasting

Zhiyong Yuan, Yumin Zhang, Yufeng Zhou*, Shanliang Dong

Science and Technology on Advanced Composites in Special Environments Laboratory, Harbin Institute of Technology, Harbin 150001, PR China

Abstract

Reaction bonded silicon carbide ceramics were successfully fabricated by gelcasting using a new non-aqueous, low-toxicity gel system based on the polymerization of phenolic-formaldehyde resin and furfuryl alcohol. Effect of solid loading on rheological properties of slurries, properties of green bodies and sintered ceramics were systematically investigated. The solid loading of suspension that can meet requirements for the casting process is as high as 70 wt.%. The drying shrinkage and green strength of the SiC/polymer network green bodies decrease with solid loading ranging from 55 wt.% to 70 wt.% due to the reduction of pre-mixed solutions . The fracture toughness and bending strength of the sintered ceramics increase with the increase of solid loading. The highest values of strength and toughness are observed at 378±16 MPa and 4.22±0.13 $MPam^{1/2}$ for the composites produced with a solid loading of 70 wt.%, respectively.

Keywords: SiC Ceramics; Gelcasting; Reaction sintering; Solid loading; Mechanical properties.

* Corresponding author. Tel.: Fax: +86 0451 86403849. Email address: zhouyf@hit.edu.cn (Y. Zhou)

1. Introduction

Due to the distinct advantages of near-net-shape forming, high dried density, low levels of organic additives, high degree of homogeneity and high dried strength, gelcasting has received a great deal of attention and has been applied to fabricate high-quality, complex-shaped ceramic parts [1-4]. In the gelcasting process, ceramic powders are dispersed into a pre-mixed solution containing a monomer, cross-linker, and solvent to form a castable slurry by ball-milling. After adding catalyst and initiator, the slurry is poured into a pore-free mold with desired shape, then the entire system is polymerized in situ to immobilize the dispersed ceramic powders in the gelled part, and green body with excellent mechanical property but only few percents of polymer is obtained. Thus, the dried green bodies can be easily machined.

Up to now, acrylamide (AM) is the most widely used gel monomer in gelcasting of ceramics. However, industry has been reluctant to use AM because it is a neurotoxin, and its polymerization is inhibited by oxygen [5, 6]. Therefore, searching for a low or nontoxicity gel-forming system that can still provide mechanical properties similar to the AM-based system has become a focused area of research in the field for more than 10 years [7-11]. In our previous work [12], a new non-aqueous gelcasting system consisting of phenolic-formaldehyde resin (PF) and benzenesulfonyl chloride was developed for the casting of reaction bonded silicon carbide ceramics. Ethylene glycol was used as the solvent, and furfuryl alcohol (FA) to modify the polymerization of the gelcasting. Additionally, porous carbons derived from the pyrolysis of the resin-glycol mixtures were used as the carbon source. The gel time was modified by changing

furfuryl alcohol/phenolic resin mass ratio and curing catalyst content in the pre-mixed suspensions, and the viscosity of the SiC suspensions was modified by varying the amount of dispersant (PEG400).

However, the green body shows large drying shrinkage during curing and carbonization. In general, a large shrinkage of the green body tends to cause deformation or cracking especially in complex shaped parts [13, 14]. Moreover, the sintered bodies have a relatively high volume fraction of free silicon. For the case of reaction bonded silicon carbide, the residual silicon that exists inside the residual pores is known to have a detrimental effect on the mechanical properties and reliability [15, 16], indicating that strength and fracture toughness of silicon are <100 MPa and <1 MPa · $m^{1/2}$, respectively.

The primary purpose of this work is to prepare reaction bonded silicon carbide ceramics with complex shape and a lower amount of residual silicon based on gelcasting and reaction sintering. The effects of blend ratio and solid loading on the rheological behavior of non-aqueous SiC-resin slurries are investigated. Microstructure and mechanical properties of the green and sintered samples are also evaluated.

2. Experimental

2.1 *Sample preparation*

The starting materials and flow chart of gelcasting process have been illustrated in our previous work [12]. Two commercial α-SiC powders A and B (Purity 98.5%, Huanyu, Zibo, China) with particle sizes of 3 μm and 45 μm were used as the raw materials. Polymeric components used in this study as binder as well as additional

carbon source were PF and FA. In addition, ethylene glycol was used as a fugitive phase and the solvent. Polyethylene glycol 400 (PEG400) were chosen as the dispersant. The raw powders together with 1.0 wt.% PEG400 were added to the pre-mixed solution of PF, FA and EG, followed by ball milled using silicon carbide balls. The initial milling was conducted for 20 h using a planetary ball mill (QM-3SP4, Nanjing NanDa Instrument Plant, China) with rotational speed of 240 r/min. Then benzenesulfonyl chloride (curing catalyst) was added into the suspension and a further ball milling for another 2 h was made. The slurry was degassed for 15 min in a rotary evaporation (TP-08, Beijing Orient Sun-Tec Co. Ltd., Beijing, China) before poured into a nonporous plaster mold. After pre-cured at 80 $^{\circ}$C for 2 h, the rigid body was subsequently cured at 150 $^{\circ}$C for 16 h and pyrolyzed by heating up to 800 $^{\circ}$C at a programmed heating rate of 2 $^{\circ}$C /min in flowing N_2. At last, the obtained green body was sintered by liquid silicon infiltration at 1700 $^{\circ}$C for 30 min in vacuum.

2.2 ***Measurements***

The rheological behaviors of the concentrated suspensions after ball milled at 240 rpm for 20 h were measured by a strain-controlled rotation rheometer (Model NXS-11, Chendu Instrument Plant, P.R.China) at room temperature. Couette (cup diameter: 36.8mm; bob diameter: 35.0mm; bob length: 37.3mm) was used for all these measurements. In order to avoid undesired influence from different mechanical histories, all samples were preconditioned at a shear rate of 50 S^{-1} for 1 min and left standing for additional 1 min before collecting the data. Microstructure of the polished and fracture surfaces was observed with laser scanning confocal microscope (OLS3100, OLYMPUS,

Japan) and scanning electron microscopy. Pore structure of the bodies after pyrolyzed was examined by a mercury porosimeter (PoreSizer 9500, 2020M, Micromeritics, USA). Before measurement, all samples were degassed under vacuum at 200 °C for 3 hours.

Bulk density of the sintered samples was determined by Archimedes principle. The composition of the specimens was analyzed by X-ray diffraction (XRD, Dmax-rb, Rigaku, Japan) using Cu Kα radiation. The scanning rate was 2◦ min^{-1} and the scanning angles ranged from 20° to 80° with a sampling width of 0.02°. Flexural strength(s) of the green and sintered bodies was measured by using three-point bending test (Model5569,Instron, USA) on 36 mm×4 mm×3 mm test bars, using a loading span of 30 mm with a cross head speed of 0.5 mm/min at room temperature. Fracture toughness of the sintered body was evaluated using single-edge notched bend beams 22 mm×4 mm×2 mm, with a notched depth and width of 2 mm and 0.2 mm, respectively, using a span of 16 mm and a cross head speed of 0.05 mm/min. A minimum number of five specimens were tested for each experimental condition.

3. Results and discussion

3.1 Rheological property of SiC suspension

3.2.1 Effect of blend ratio

Preparation of stable high solid-loading ceramic suspension, with a low viscosity, still is a prerequisite for successful application of gelcasting. The particle size distribution will influence the packing ability of the powders within a suspension by modifying the arrangement of the particles with the finer particles filling the void space between the larger one and hence, determine the rheological properties of the

suspension. The use of bidisperse suspensions can provide two advantages [17-19]. One is that, at a given solid volume fraction, the viscosity of a bidisperse suspension is generally lower than that of a monodisperse suspension. The other is that, for a desirable viscosity value, the use of a bidisperse suspension can attain a higher solid volume fraction than the use of a monodisperse suspension.

Fig. 1 illustrates the effect of the blend ratio of SiC powders on the equilibrium viscosity of the suspensions with a constant solid loading of 60 wt.% and dispersant content of 1.0 wt.%. The suspensions containing high proportion of SiC B (coarser powder) show lower viscosity value at shear rates below 10 s^{-1}. The viscosity values gradually decrease as more SiC A are replaced by SiC B, reaching a minimum when the volume fraction of SiC B reaches 80 %. But at shear rates greater than 10 s^{-1}, suspensions with blend ratio of 70 % shows the lowest viscosity. Many experimental and theoretical findings [20-22] have shown that, when solid loading and the diameter ratio of large to small particle are fixed, there exists a critical value of blend ratio at which the viscosity is minimized.

Furthermore, Fig. 1 also shows that the suspensions all display a shear thinning behavior with an approach to a plateau at high shear rates. At low shear rates, the suspension structure is close to the equilibrium structure at rest because thermal motion dominates over the viscous force [23]. At higher shear rates, the viscous forces affect the suspension structure more, and shear thinning occurs. Shear thinning behavior generally indicates that the flow can induce a more favorable two-dimensional layered structure arrangement of the particles because flow-induced layered arrangement can

decrease the resistance of particle movement between different layers [23]. At very high shear rates, the viscous forces dominate, and the plateau in viscosity in this region is a measure of the resistance to flow of a suspension with a completely hydrodynamically controlled structure.

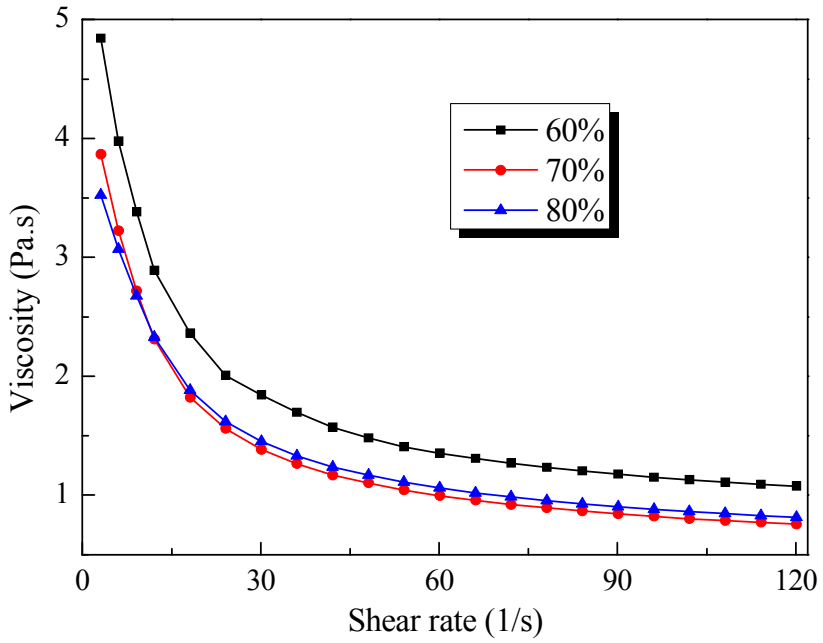

Fig. 1. Steady shear viscosity for two-component SiC suspensions with different weight fraction of SiC B.

3.2.2 Effect of solid loading

A suspension for gelcasting should always meet two requirements [24]: good fluidity and high solid loading. On the one hand, a suspension with good fluidity has uniform structure and ensures that the slurry can be poured into mold successfully; on the other hand, higher solid content can result in higher density as well as less deformation and defects of the green and sintered parts. Fig. 2 shows the viscosity vs. shear rate for SiC-resin slurries with different solid loading. Viscosity of all the slurries descends while shear rate ascends. With 55 wt.% solid loading, the viscosity is

approximately 780 mPa s at 60 s^{-1}. As the solid loading increases, the viscosity corresponds to it. The viscosity for the slurries with 60 wt.%, 65 wt.%, 70 wt.% and 75 wt.% solid loading is 1.0 Pa s, 1.58 Pa s 3.57 Pa s and 7.35 Pa s, respectively.

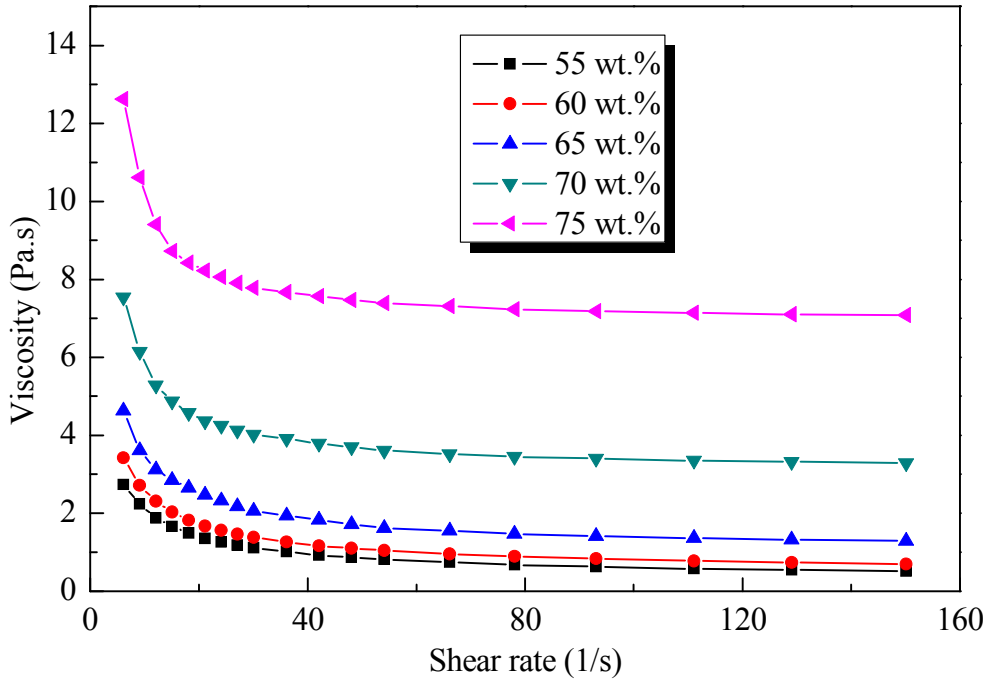

Fig. 2. Properties of SiC suspensions with different solid loading.

In gelcasting process, preparation of high solid loading slurries is a key issue because higher solid loading could reduce the shrinkage during curing and carbonization and reduce the possible cracks and inhomogeneity. Fortunately, the viscosity of slurry with a high solid loading up to 70 wt.% is still meeting the demands of the following gelcasting process.

3.2 *Characterization of green bodies*

The relative shrinkage of green bodies versus the solid loading in slurries is shown in Fig. 3. The relative shrinkage of green pieces during curing decreases with the

descending of the solid content, reduces from 10.2 % at 55 wt.% to 5.6 % at 75 wt.%. Meanwhile, the shrinkage of the green bodies during carbonization also decreases from about 2.4 % to 0.2 %.

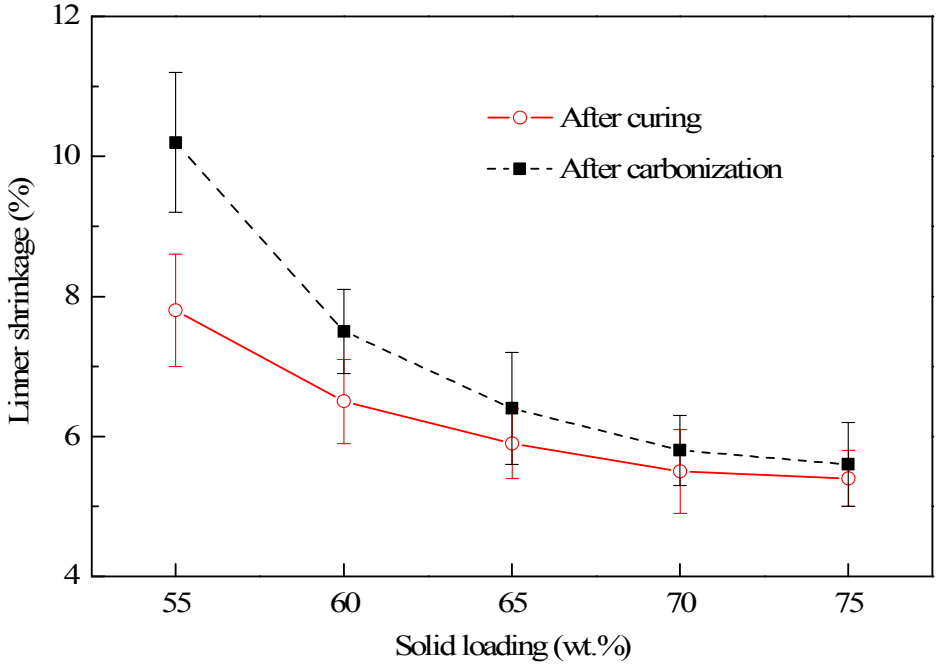

Fig.3 Effect of solid loading on linear shrinkage of the green bodies

After cast into a mold at constant temperature of 70 ^{o}C, SiC/resin suspensions were consolidated within 10 min, and well-shaped green bodies without surface exfoliation layer are obtained. The mechanical properties of the green pieces with different solid loading are showed in Fig. 4. The green mechanical properties are significantly improved with respect to those obtained by conventional forming procedures, such as slip casting, tape casting and some gel-casting procedures [25-27], so that the green parts can be easily handled and machined in the green state. The high strength comes from the cross-linking gel network and the homogenous packing of particles. The flexural strength of the green bodies gradually decreases from 21.2±1.9 MPa to 12.7±

1.5 MPa as the solid loading increases from 55 wt.% to 70 wt.%. With increased solid loading, polymer networks are used to keep more SiC particles together, thus the crosslink of powders is weakened, which results in the decrease of green strength. When the solid loading is 75 wt.%, however, the green mechanical property shows a sharp decrease. This might be due to the existence of several pores of a few hundred micrometers level, as shown in Fig. 5, which is not observed in the green bodies with lower solid loading. When solid loading is too high, gases in the slurry cannot be easily removed due to its high viscosity.

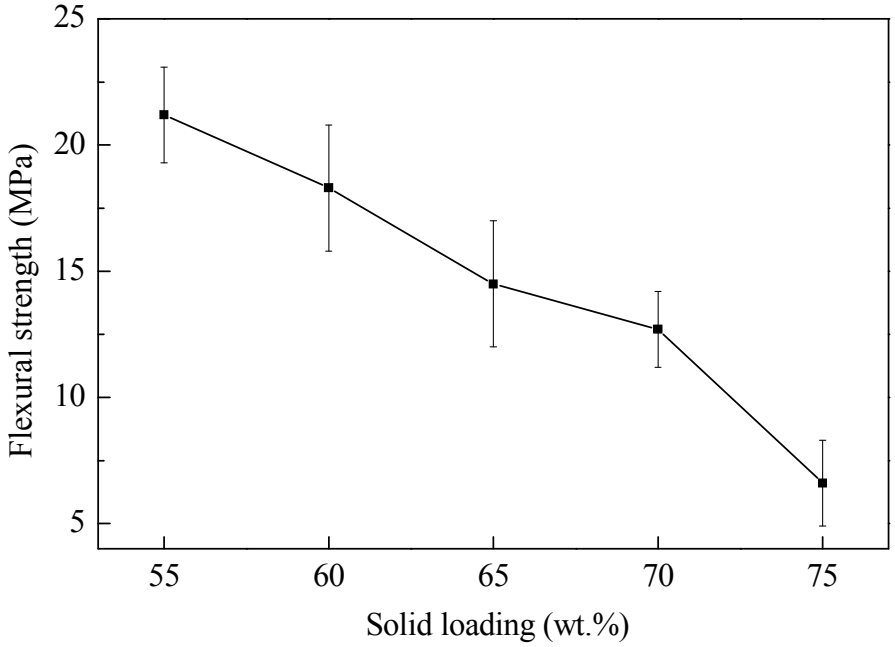

Fig.4. Flexural strength of the cured bodies as a function of solid loading.

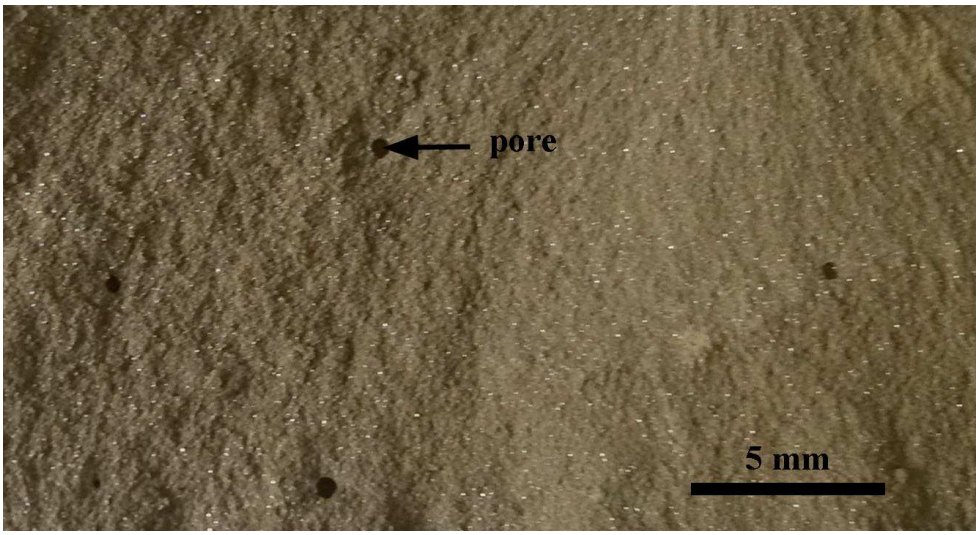

Fig. 5 Fracture morphology of the green bodies with a solid loading of 75 wt.%.

The fracture surface of the green bodies is examined by SEM. From the microstructure shown in Fig. 6, homogeneous structure with no obvious flaw, crark or bubble could be obtained, suggesting that well-dispersed slurry, good deairing and casting could be achieved by the new gelcasting system. SiC powders are connected by polymer networks, as shown by red arrows, which present the green body's high strength. With solid loading increased from 55 to 70 wt.%, thickness of the polymer networks covered on SiC powders decreases obviously. An analysis of the polymer networks shows that there are many interconnected pores of nanometer level, as depicted in the inset of Fig. 6. Thus, we believe that phase separation occurred in the course of polymerization of PF and FA, with only two phases being evident in the premixed solutions, a polymeric resin-rich phase and an ethylene glycol-rich phase [28]. After curing and carbonization, the polymeric resin-rich phase became carbon matrix and the ethylene glycol-rich phase was removed to leave pores in the carbon matrix.

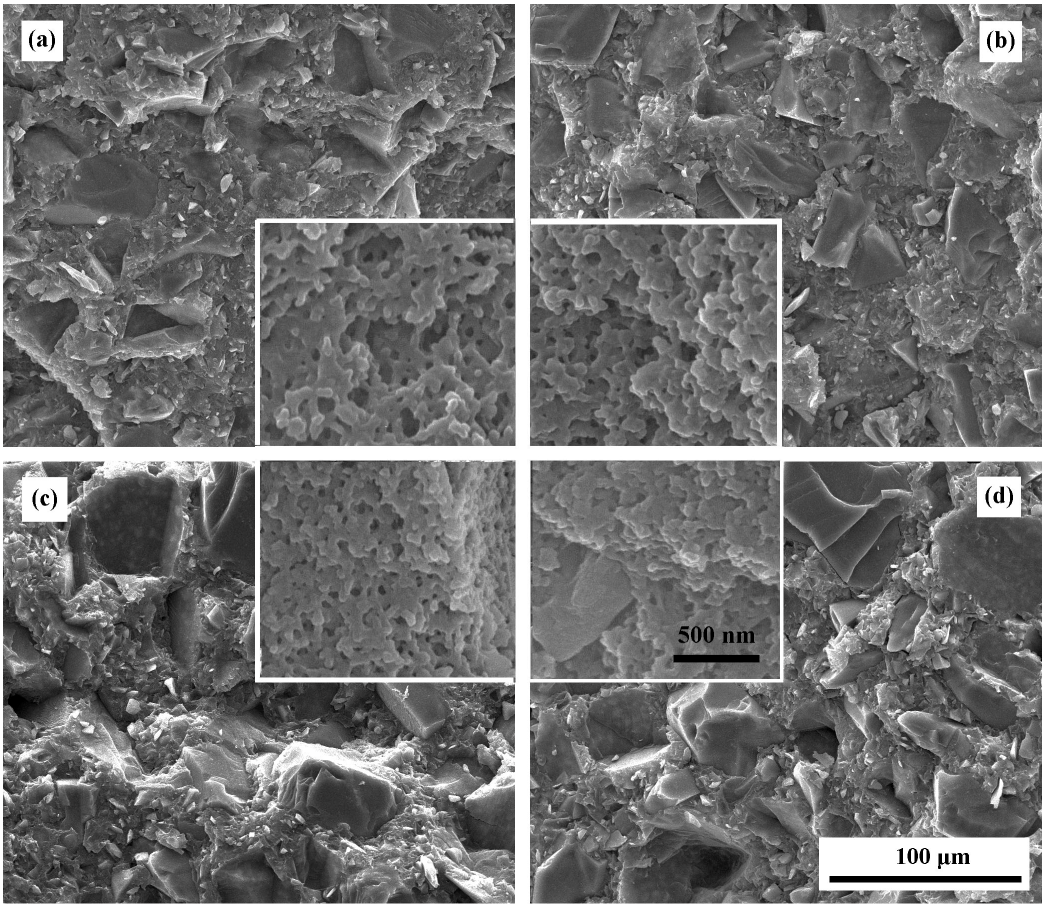

Fig. 6. Micrograph of the fractured surface of the green bodies with different solid loading: (a) 55 wt.%, (b) 60 wt.%, (c) 65 wt.%, (d) 70 wt.%.

After carbonization at 800 ˚C for 0.5 h in flowing nitrogen, the pore size distribution of the SiC/porous carbon samples with different solid content was obtained by Hg intrusion porosimetry. As shown in Fig. 7, the pore size shows a monomodal distribution type. Single peak distribution of pore size indicates that SiC/porous carbon bodies have a homogeneous structure. The pore size distributions of all samples are almost equal and very narrow, and most of pores ranging from 90 to 30 nm. According to Xu [29], pore structure of the porous carbon monoliths produced by polymerization-induced phase separation is defined by the ingredients of the premixed solutions and the thermal history of the polymer system. Moreover, the maximum

distribution of pore size in green pieces decreases with the ascending of solid content of the slurries.

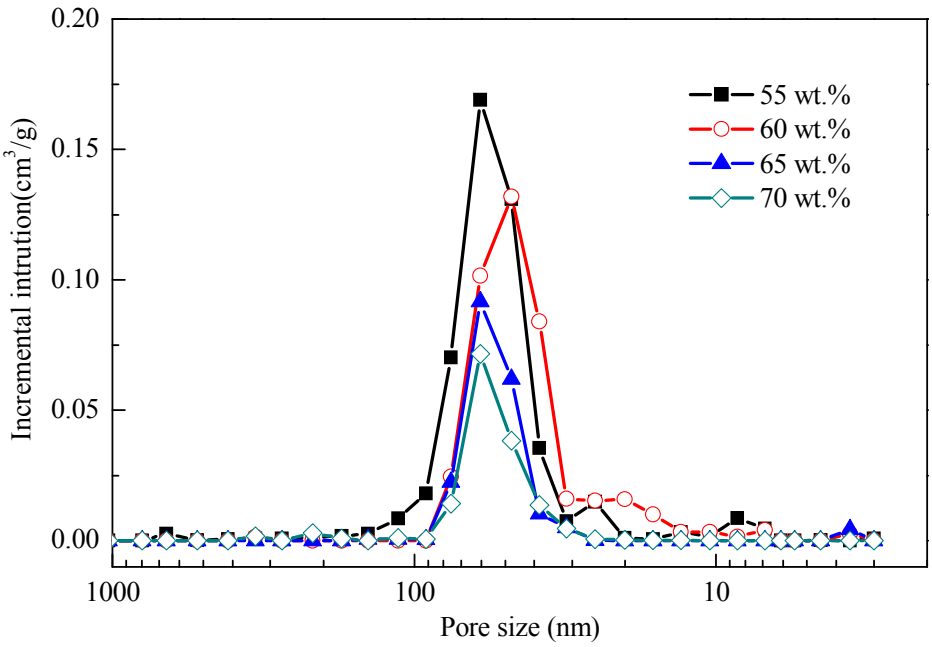

Fig.7. Pore size distribution of SiC/porous carbon bodies with different solid content.

Bulk density and apparent porosity of the SiC/porous carbon bodies with different solid loading was obtained by Hg intrusion porosimetry, and the results are shown in Fig. 8. As the solid loading increases from 55 wt.% to 70 wt.%, the bulk density of the carbonized bodies increases from 1.30 g/cm^3 to 1.63 g/cm^3, while the apparent porosity decreases from 32 % to 25.2 % . Higher solid loading could lead to higher green density and lower apparent porosity, which is mainly due to the packing behavior of the bimodal SiC particles and the amount of porous polymer networks.

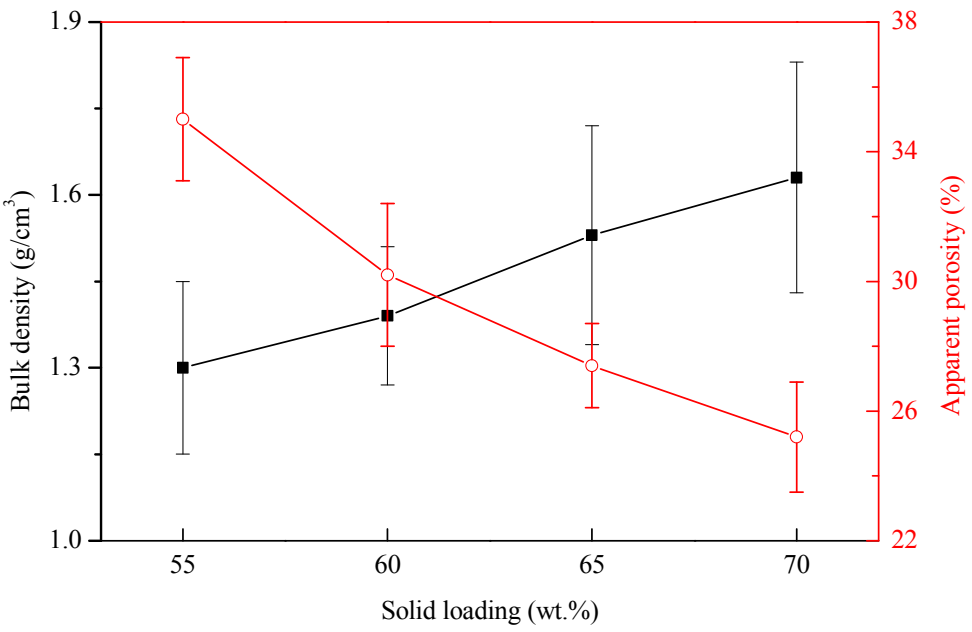

Fig. 8. Bulk density and apparent porosity of the green bodies as a function of solid loading

3.4 *Characterization of sintered pieces*

After machined in the green state, carbonization and reaction sintering, complex-shaped RBSC ceramic parts can be produced. From the optical microscope image in Fig. 9, the SiC/porous carbon bodies with different solid loading were all completely infiltrated by liquid silicon at vacuum, showing a dense polished surface, indicating that the excessive pores were fully filled by residual Si after the siliconization reaction. Relative homogeneous distribution could be observed, and neither residual carbon (black color parts) nor large area of silicon is found. As a result, the fraction of residual Si is determined by the porosity of the green body. In the image, the parts of gray color represent the original α-SiC and newly formed β-SiC particles and those of the white color indicate silicon. The pores between particles are filled with silicon.

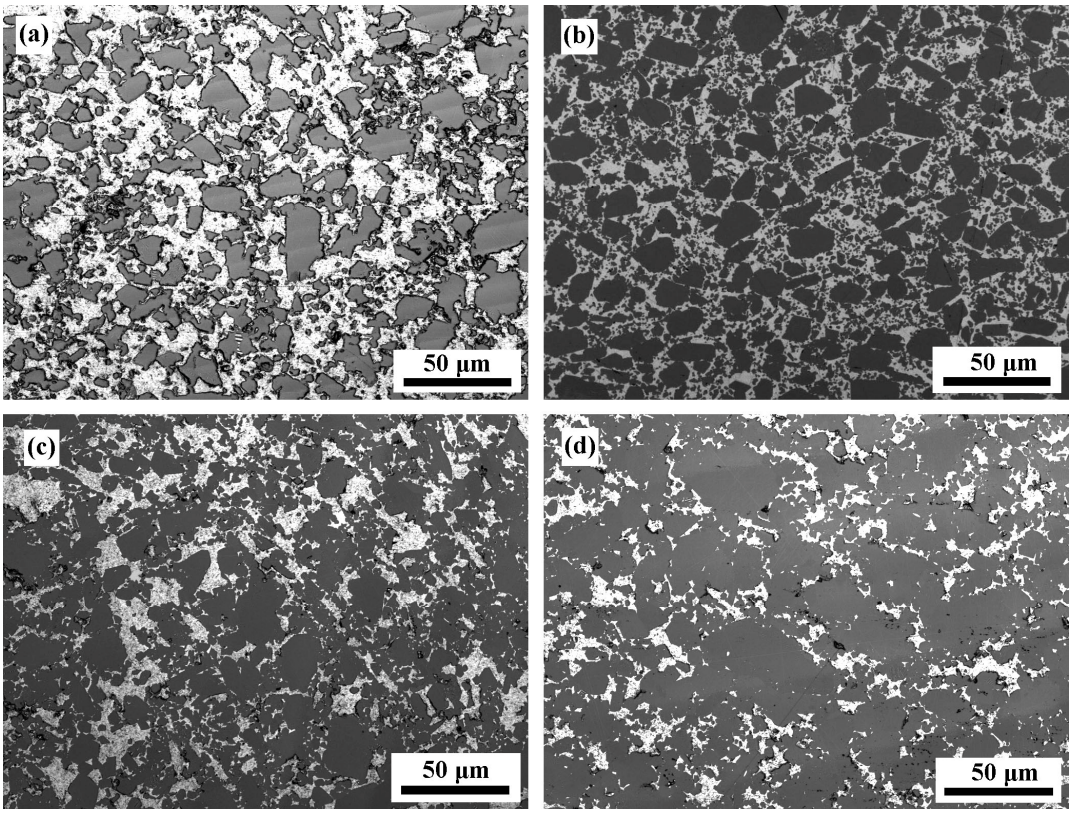

Fig.9 Morphology of the polished surface of RBSC with the solid loading : (a) 55 wt.%, (b) 60 wt.%, (c) 65 wt.%, (d) 70 wt.%.

Phase composition was determined by XRD patterns. The XRD analysis was conducted on the polished surface. Fig. 10 shows the XRD patterns of the materials with different solid loading. The sintered ceramics are composed of three main phases α-SiC, β-SiC and Si; whereas C phase is not detected. The specimens with higher solid loading have lower fraction of Si phase derived from the strongest peaks intensity of Si among the four specimens. Such a variation of silicon content is compatible with the bulk density change of the carbonized samples in Fig. 9. The low content of Si here is explained by the reduced porosity in SiC/porous carbon bodies. The density of SiC and Si are 3.21 and 2.34 g/cm^3, respectively. For the high densification of RBSC, variation of Si fraction in the composite implies variation of bulk density. The bulk density as a function of solid loading is listed in Table. 1. The density increases with solid loading in

the range of 55–70 wt.%.

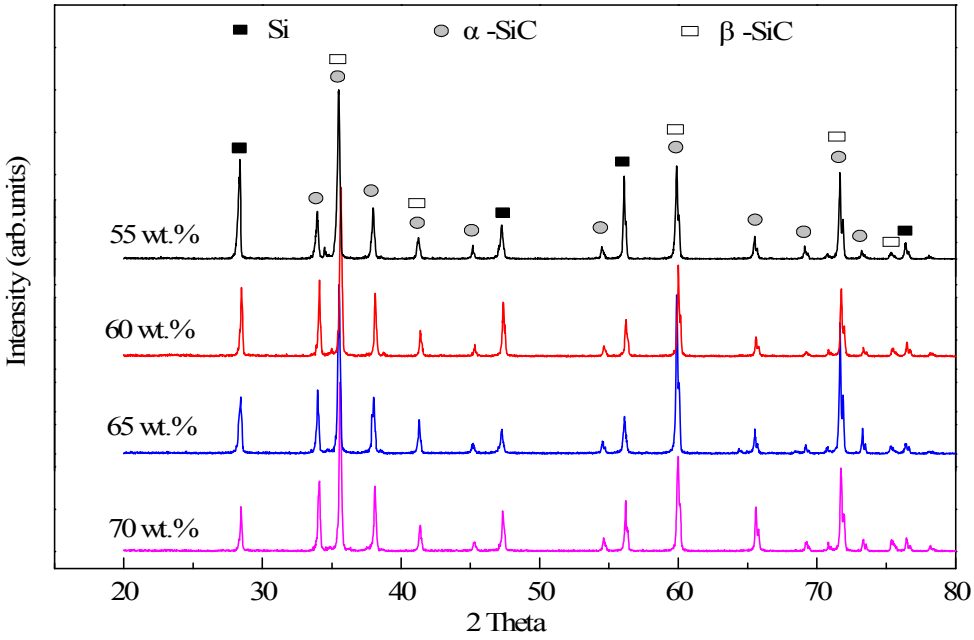

Fig. 10. Composition of the SiC ceramic.

Table1

Properties of the sintered bodies.

Sample	Bulk density ($g.cm^{-3}$)	Silicon content (%)	Flexural strength (MPa)	Fracture toughness ($MPam^{1/2}$)
SC-55	2.94	31.0	244±15	3.08±0.15
SC-60	3.00	24.1	262±18	3.37±0.19
SC-65	3.04	19.5	300±20	3.87±0.19
SC-70	3.06	17.2	358±16	4.22±0.13

The fracture surface of the sintered SiC ceramics is shown in Fig. 11. Based on the SEM micrograph, the intergranular fracture of SiC is the main fracture mode, coupled with the brittle fracture of residual silicon. The flexural strength and fracture toughness of the as-prepared SiC ceramics with different solid loading are presented in Table. 1. The flexural strength and fracture toughness both increase dramatically with solid

loading, and when the solid loading is 70 wt.%, the sintered body exhibits the highest bending strength and fracture toughness which are 358±16 MPa and 4.22±0.13 MPam$^{1/2}$, respectively.

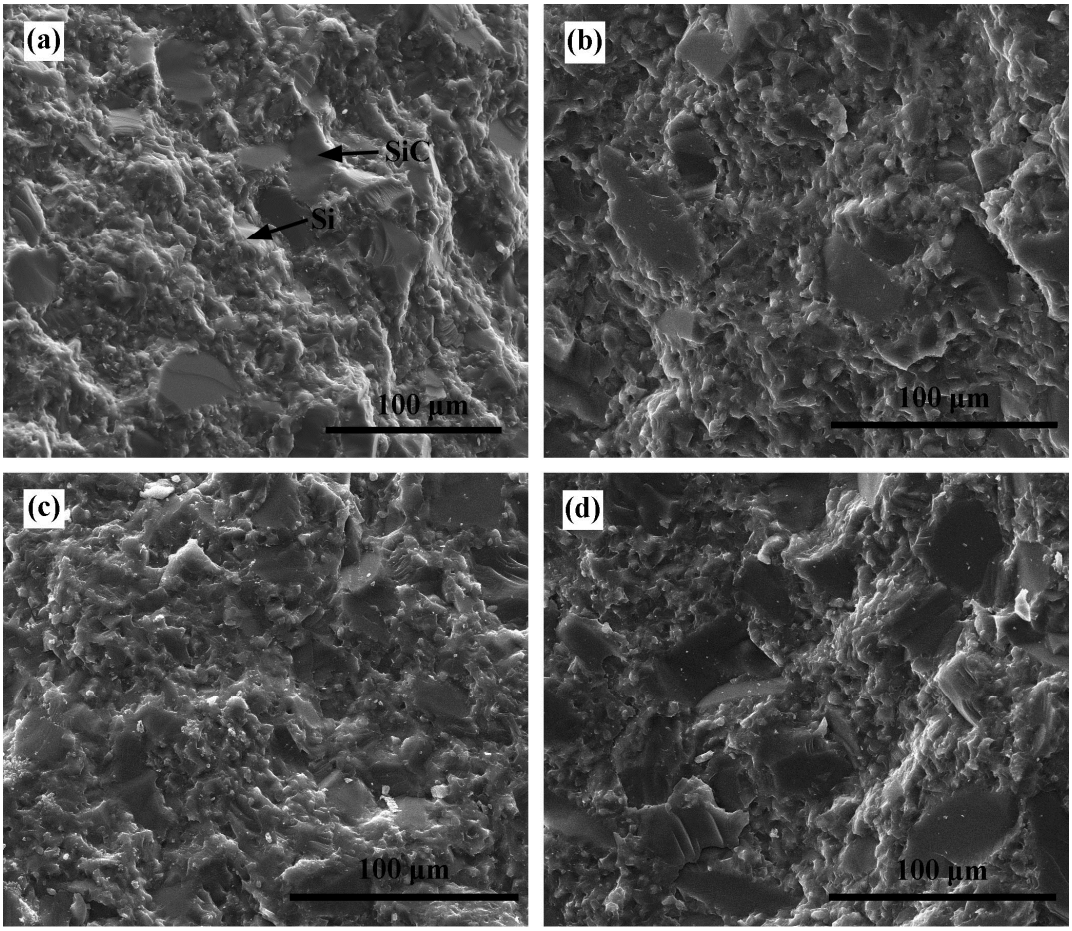

Fig. 11. Morphologies of the fractural surface of the SiC ceramic with different solid loading: (a) 55 wt.%, (b) 60 wt.%, (c) 65 wt.%, (d) 70 wt.%.

4. Conclusions

PF combined with FA was developed to consolidate suspensions to manufacture silicon carbide ceramics. A discussion of experimental data leads to the following conclusion:

1. Slurries with high solid loading and low viscosity were prepared by using PEG400

as dispersant and optimizing particle size distribution.

2. When the solid loading is lower than 75 wt.%, the bending strength of the green body is higher than 10 MPa (because SiC particles are maintained in a three-dimensional polymer network), which could satisfy the requirement of machining.
3. With the increase of solid loading, the bulk density, bending strength and fracture toughness increased. The sintered bodies with solid loading of 70 wt.% show the largest bending strength and fracture toughness of 358±16 MPa and 4.22±0.13 MPam1/2, respectively.
4. When the solid loading was increased to 75 wt.%, gases in the slurry which could not be easily removed due to its high viscosity appeared in the cured bodies, which resulted in the decrease of green strength.

Acknowledgements

This work was supported by Major State Basic Research Development Program of China (2014cb046505) and Research Fund for the Doctral Program of Higher Education of China (20132302120022).

References

[1] Young AC, Omatete OO, Janney MA, Menchhofer PA. Gelcasting of alumina. *J Am Ceram Soc* 1991; 74[3]: 612-8.

[2] Yang J, Yu J, Huang Y. Recent developments in gelcasting of ceramics. *J Eur Ceram Soc* 20011;31:2569-91.

[3] He R, Hu P, Zhang X, Liu C. Gelcasting of complex-shaped ZrB2-SiC ultra high

temperature ceramic components. *Mat Sci Eng A* 2012; 556:494-9.

[4] Zhang C, Huang X, Yin Y, Xia F, Dai J, Zhu Z. Preparation of boron carbide–aluminum composites by non-aqueous gelcasting. Ceram Int 2009;35:2255-9.

[5] Sepulveda P, Binner JGP. Evalution of the in situ polymerization kinetics for the gelcasting of ceramic foams. *Chem Mater*, 2001; 13:3882-7.

[6] Li F, Chen H, Wu R, Sun B. Effect of polyethylene glycol on the surface exfoliation of SiC green bodies prepared by gelcasting. *Mat Sci Eng A* 2004; 368:255-9.

[7] Chen B, Jiang D, Zhang J, Dong M, Lin Q. Gel-casting of α-TCP using epoxy resin as a gelling agent. *J Eur Ceram Soc* 2008;28:2889-94.

[8] Jia Y, Kanno Y, Xie ZP. Fabrication of alumina green body through gelcasting process using alginate. *Mater Lett* 2003;57:2530-4.

[9] Wan W, Yang J, Zeng J, Yao L, Qiu T. Aqueous gelcasting of silica ceramics using DMAA. *Ceram Int* 2014;40:1257-62.

[10] Potoczek M. Hydeoxyapatite foams produced by gelcasting using agarose. *Mater Lett* 2008;62:1055-7.

[11] Millan AJ, Nieto MI, Moreno R. Aqueous gel-forming of silicon nitride using carrageenans. *J Am Ceram Soc*, 2001;84:62-4.

[12] Zhang Y, Yuan Z, Zhou Y. Gelcasting of silicon carbide ceramics using phenolic resin and furfuryl alcohol as the gel former. *Ceram Int* 2014;40:7873-8.

[13] Zhang C, Qiu T, Yang J, Guo J. The effect of solid volume fraction on properties of ZTA composites by gelcasting using DMAA system. *Mat Sci Eng A* 2012;539:243-9.

[14] Wan W, Yang J, Zeng J, Yao L, Qiu T. Effect of solid loading on gelcasting of silica

ceramics using DMAA. *Ceram Int* 2014;40:1735-40.

[15] Kumar RS, Sivakumar D, Venkateswarlu K, Gandhi AS. Mechanical behavior of molybdenum disilicide reinforced silicon carbide composite. *Scripta Mater* 2011;65:838-41.

[16] Dai PY, Wang YZ, Liu GL, Wang B, Shi YG, Yang JF, et al. Fabrication of highly dense pure SiC ceramics via the HTPVT method. *Acta Mater* 2011;59:6257-60.

[17] Zaman AA, Moudgil BM. Rheology of bidisperse aqueous silica suspensions: a new scaling method for the bidisperse viscosity. *J Rheol* 1998;42: 21-39.

[18] Ferreira JMF, Diz HMM. Pressure slip casting of bimodal silicon carbide powder suspension. *Ceram Int* 1999;25:491-5.

[19] Aroati S, Cafri M, Dilman H, Dariel MP, Frage N. Preparation of reaction bonded silicon carbide (RBSC) using boron carbide as an alternative source of carbon. *J Eur Ceram Soc* 2011;31:841-5.

[20] Dames B, Morrison BR, Willenbacher N. An empirical model predicting the viscosity of highly concentrated, bimodal dispersions with colloidal interactions. *Rheol Acta* 2001;40:434-40.

[21] Logos C, Nguyen QD. Effect of particle size on the flow properties of a south Australian coal–water slurry. *Powder Techno* 1996;88:55-8.

[22] Huang Q, Li W, Gu M, Chen P, Zhang H, Qin Y. Effect of blend ratio on rheological properties of aqueous SiC suspensions. *J Eur Ceram Soc* 2004;24:2157-61.

[23] Bergstrom L. Shear thinning and shear thickening of concentrated ceramic suspensions**.** *Colloid Surface A* 1998;133:151-5.

[24] Ankur G, Ankit K, Balashanmugam N, Arun MV, Giridhar M. Optimization of rheological properties of photopolymerizable alumina suspensions for ceramic microstereolithography. *Ceram Int* 2014; 40:3655-65.

[25] Li Y, Lin J, Gao J, Qiao G, Wang H. Fabrication of reaction-bonded SiC ceramics by slip casting of SiC-C suspension. *Mat Sci Eng A* 2008483-484:676-8.

[26] Luo ZH, Jiang DL, Zhang JX, Lin QL, Chen ZM, Huang ZR. Preparation of reaction-bonded silicon carbide with well controlled structure by tape casting method. *Ceram Int* 2012;38:2125-8.

[27] Wang X, Xie ZP, Huang Y, Cheng YB. Gelcasting of silicon carbide based on gelation of sodium alginate. *Ceram Int* 2002;28:865-71.

[28] Yuan Z, Zhang Y, Zhou Y, Han J. Preparation and characterization of porous carbons obtained from mixtures of furfuryl alcohol and phenol-formaldehyde reisn. *Mater Chem Phys* 2014;143:707-12.

[29] Xu S, Li J, Qiao G, Wang H, Lu T. Pore structure control of mesoporous carbon monoliths derived from mixtures of phenol resin and ethylene glycol. *Carbon* 2009;47[8]:2101-11.